A Successive Linear Programming Approach to Solving the IV-ACOPF

Anya Castillo, *Student Member, IEEE*, Paula Lipka, *Member, IEEE*, Jean-Paul Watson, *Member, IEEE*, Shmuel S. Oren, *Fellow, IEEE*, and Richard P. O'Neill, *Member, IEEE*

***Abstract*—Improved formulations of and solution techniques for the alternating current optimal power flow (ACOPF) problem are critical to improving current market practices in economic dispatch. We introduce the IV-ACOPF formulation that unlike canonical ACOPF formulations–which represent network balancing through nonlinear coupling–is based on a current injections approach that linearly couple the quadratic constraints at each bus; yet, the IV-ACOPF is mathematically equivalent to the canonical ACOPF formulation. We propose a successive linear programming (SLP) approach to solve the IV-ACOPF, which we refer to as the SLP IV-ACOPF algorithm. The SLP IV-ACOPF leverages commercial LP solvers and can be readily extended and integrated into more complex decision processes, e.g., unit commitment and transmission switching. We demonstrate with the standard MATPOWER test suite an acceptable quality of convergence to a best-known solution and linear scaling of computational time in proportion to network size.**

***Index Terms*—Alternating current optimal power flow (ACOPF), optimal power flow (OPF), rectangular coordinates, successive linear programming (SLP).**

NOMENCLATURE

A. Sets

$\mathcal{N}$	Set of buses $\{1,\ldots,N\}$
$\mathcal{K}$	Set of lines $\{1,\ldots,K\}$
$\mathcal{A}(n)$	Set of buses that are adjacent to node n
$\mathcal{F}$	Set of flows $\{1,\ldots,2K\}$

Manuscript received December 09, 2014; revised March 25, 2015 and July 27, 2015; accepted September 25, 2015. Date of publication October 16, 2015; date of current version May 02, 2016. This work was supported in part by the National Science Foundation Graduate Research Fellowship DGE 1106400 and in part by the U.S. Department of Energy's Office of Advanced Scientific Computing Research . Sandia National Laboratories is a multi-program laboratory managed and operated by Sandia Corporation, a wholly owned subsidiary of Lockheed Martin Corporation, for the U.S. Department of Energy's National Nuclear Security Administration under Contract DE-AC04-94-AL85000. Paper no. TPWRS-01680-2014.

A. Castillo is with Johns Hopkins University, Baltimore, MD 21218 USA, and also with the Federal Energy Regulatory Commission (FERC), Washington, DC 20426 USA (e-mail: anya.castillo@gmail.com).

P. Lipka and S. S. Oren are with University of California, Berkeley, Berkeley, CA 94720 USA (e-mail: plipka@berkeley.edu; oren@ieor.berkeley.edu).

J.-P. Watson is with Sandia National Laboratories, Albuquerque, NM 87185 USA (e-mail: jwatson@sandia.gov).

R. P. O'Neill is with Federal Energy Regulatory Commission (FERC), Washington, DC 20426 USA (e-mail: richard.oneill@ferc.gov).

Digital Object Identifier 10.1109/TPWRS.2015.2487042

B. Indices

h	Successive linear program iter(ation); $h \in \mathcal{H}$
n, m	Bus (node) indices; $n, m \in \mathcal{N}$
k	Three-phase transmission element; $k \in \mathcal{K}$
k'	Monitored flowgate; $k' \in \mathcal{K}'^{(h)} \subset \mathcal{K}$
$k\,(n,m)$	Flow on transmission element k from bus n to m; $k\,(n,m) \in \mathcal{F}$ where $k(m,n)$ denotes the flow in the opposite direction along line k, $k(n,\cdot)$ denotes withdrawals from bus n, and $k(\cdot,n)$ denotes injections to bus n
$k\,(\cdot)$	Directional flows on k; $k\,(\cdot) \in \mathcal{F}$
l	Piecewise linear segment; $l \in \mathcal{L}$

C. Variables

p_n^g	Total linearized real power generation at bus n
$p_{n,l}^g$	Linear segment l of generation at bus n
q_n^g	Reactive power generation at bus n
v_n	Voltage magnitude at bus n
v_n^{sq}	Linearization of $(v_n)^2$
v_n^r	Real part of voltage at bus n
v_n^j	Imaginary part of voltage at bus n
i_n^r	Real part of current injection at bus n
i_n^j	Imaginary part of current injection at bus n
$i_{k(n,m)}$	Current magnitude on k from bus n to m
$i_{k(n,m)}^{sq}$	Linearization of $\left(i_{k(n,m)}\right)^2$
$i_{k(n,m)}^r$	Real part of current on k from bus n to m
$i_{k(n,m)}^j$	Imaginary part of current on k from bus n to m

D. Parameters

B^{MVA}	Power base in MVA
R_k	Series resistance of line k
X_k	Series reactance of line k
G_k	Series conductance of line k
B_k	Series susceptance of line k
Y_k	Series admittance of line k; $Y_k = G_k + \mathrm{j}B_k$
G_{kn}^{sh}	Shunt conductance on line k connected to n
B_{kn}^{sh}	Shunt susceptance on line k connected to n
Y_{kn}^{sh}	Shunt admittance on line k connected to n

G_n^{sh}	Shunt conductance at bus n
B_n^{sh}	Shunt susceptance at bus n
Y_n^{sh}	Shunt admittance at bus n
τ_{kn}	Ideal transformer on the n-side of line k
$\|\tau_{kn}\|$	Transformer turns ratio on the n-side of line k
ϕ_{kn}	Phase-shifter on the n-side of line k
P_n^d	Real power demand at bus n
Q_n^d	Reactive power demand at bus n
$P_n^{\min}$	Minimum real power for generation at bus n
$P_n^{\max}$	Maximum real power generation at bus n
$Q_n^{\min}$	Minimum reactive power generation at bus n
$Q_n^{\max}$	Maximum reactive power generation at bus n
$V_n^{\min}$	Minimum voltage magnitude at bus n
$V_n^{\max}$	Maximum voltage magnitude at bus n
$I_k^{\max}$	Maximum current magnitude on line k
$V_n^{(h)}$	Step-size bound on the voltage at bus n in iter h
$C_n^{g,2}$	Quadratic cost coefficient for generation at bus n
$C_n^{g,1}$	Linear cost coefficient for generation at bus n
$C_{n,l}^{g}$	Linear segment l of the quadratic cost at bus n
P_n^g	Uniform piecewise segment length of the real power generation at bus n

I. Introduction

THE alternating current optimal power flow (ACOPF) problem, also known as the OPF, co-optimizes real and reactive power dispatch in order to promote reliable operation and efficient markets. The ACOPF originated from Carpentier's reformulation of the economic dispatch problem based on the Karush-Kuhn-Tucker conditions [1]. Identifying a globally optimal solution to the ACOPF is known to be non-deterministic polynomial-time (NP) hard [2]. Consequently, this key dispatch problem is not presently solved exactly, although doing so would address many of the operational challenges in markets today. According to Stott and Alsaç [3], there are basic requirements other than absolute optimality for practical and non-trivial applications, and the appropriate amount of detail can be elusive, if not situationally dependent.

As such, Independent System Operators (ISOs) and other grid operators use approximate solution techniques based on linear programming (LP) and mixed-integer linear programming (MILP) in order to leverage the performance of commercial LP/MILP solvers such as Gurobi and CPLEX. System operators frequently solve the direct current optimal power flow (DCOPF) problem adjusted with loss factors. The DCOPF approach holds voltage constant, ignores reactive power flows, assumes small voltage angle differences, and models resistances (R) as much less than reactances (X) on network components. Subsequently, AC feasibility is achieved through an iterative, quasi-optimization process to ensure that a realistic engineering solution is obtained by the DCOPF model and to identify constraint violations that may require preventive actions including re-dispatch, reactive power compensation, and voltage support. Some system operators solve a decoupled OPF model, which iterates between P–Θ and Q–V subproblems in order to achieve AC feasibility. As a result, dispatches and prices are most often obtained within the required time limits, but such approximations can be inaccurate when the system is stressed or when there is a strong physical coupling between real and reactive power.

The DCOPF and decoupled OPF approaches oversimplify the physical problem and require operator intervention in the day-ahead, intra-day, and real-time markets. Purchala *et al.* [4] demonstrate that the DCOPF approach is acceptable if the voltage profile is sufficiently flat, the R/X ratio of transmission lines is less than 0.25, and the network is not heavily loaded. Consequently, the system model which is used to clear the market may not be able to physically dispatch the resources that are required to satisfy constraints, such as voltage limits, that are not accurately reflected in the market software. Moreover, the Midwest Independent System Operator (MISO) intervenes at times in load pockets in order to commit units for voltage and local reliability requirements; producing voltage and reactive power schedules without compromising MW transmission line limits (security) and efficiency would require ACOPF constraint modeling [5]. A report to congress prepared by the United States Department of Energy (DOE) states: "the technical quality of current economic dispatch tools-software, data, algorithms, and assumptions-deserves scrutiny. Any enhancements to these tools … will improve the reliability and affordability of the nation's electricity supplies" [6]. Given the cost of upgrading existing ISO market software is less than $10 million dollars [7] and small increases in dispatch efficiency can yield billions of dollars per year in cost savings[8], the potential benefit-to-cost ratio of improved market software is at least 100 fold.

The computational tractability and convexity of any solution approach is critical to support market clearing strategies based on the locational marginal price (LMP), which is the marginal cost of supplying the next MW of load at a particular location in time and accounts for the next incremental unit of energy, network congestion, and transmission losses. LMPs are derived from the shadow price on nodal real power balancing constraints in the optimization model and reflect loop flow through conserving Kirchhoff's laws. In the DCOPF and decoupled OPF models, the LMP is highly dependent on the aforementioned modeling assumptions. Without transparency into the exact form of the problem solved in the markets, it is difficult to assess to what extent price signals are ensuring efficient and reliable operations. In 2009, Liu *et al.* [9] reported that full derivations of the LMP are not available in ISO tariffs and other publicly available manuals. Furthermore, the clearing prices in current markets do not reflect the true marginal cost of production, which subsequently results in uplift. A central challenge in accounting for better physical and operational constraints is to apply better representations of the underlying AC power system in the market software [10].

Efforts to incorporate all physical and operational constraints have been tracked with over half a century of work on load flow and ACOPF formulations, decomposition methods, and

algorithms; please see[8], [11]–[18] for comprehensive surveys. Kirchhoff's laws impose nonconvex constraints through the products of unknown bus voltages, which are represented in either polar or rectangular coordinates, or both [19]. Both power injection [20] and current injection [21] formulations have been developed to solve the load flows. When rectangular coordinates with current injections are applied to determine the load flow, the network balancing becomes a linear system of equations. We apply this load flow approach in the formulation of the IV-ACOPF problem, which is expressed in current-voltage equations and extends the initial concepts presented in [22]. The IV-ACOPF is equivalent to the canonical ACOPF formulations, as we demonstrate in [23].

In this paper we present the IV-ACOPF problem and propose a successive linear program (SLP) approach to solve the IV-ACOPF. We apply first-order Taylor series expansions to construct local subproblems, and apply a combination of outer approximation and constraint reduction techniques. We iteratively co-optimize real and reactive power dispatch and do not introduce binary variables in our approach. Our approach can be extended to include discrete controls and can be embedded within branch-and-bound algorithms to support more complex decision processes, including unit commitment and transmission switching. Since ISO market software depends on commercial LP/MILP solvers, our proposed approach is suitable for such applications, the solution is tractable, and the LMPs are recoverable. We demonstrate an acceptable quality of convergence to the best-known solution and linear scaling of computational time in proportion to network size as compared to the reported non-linear programming (NLP) approaches. These performance characteristics may be accessible in real-world applications.

The remainder of this paper is organized as follows. In Section II we provide a literature review of seminal and recent linearization and convexification techniques for the ACOPF. In Section III we summarize our SLP algorithm and in Section IV we formulate the IV-ACOPF and the local subproblem of the SLP. In Section V we demonstrate the computational performance and convergence quality of our SLP IV-ACOPF algorithm. We conclude in Section VI with a brief discussion of our results.

II. Related Work

Most LP approaches take advantage of the loose coupling between voltage angle and magnitude, as initially proposed by Alsaç and Stott [24], which can be difficult to resolve if the system has high losses, is highly loaded, or either subproblem is infeasible. Kirschen and Meeteren [25] propose an improved method which reschedules real power controls in order to correct voltage magnitude violations that arise in the decoupled subproblem. However, when a high physical coupling in P–Q exists, even such reschedules can be ineffective.

Coupled models, such as the one proposed in this work, respect bus voltage limits and reactive power requirements during MW scheduling. Although the decoupled model has smaller subproblems in each iteration, the coupled version can take fewer iterations and be faster overall depending upon the linearization and underlying network [26]. Other coupled models include the recent works described in [27]–[29]. Franco *et al.* [27] apply a least-squares regression to obtain a non-iterative linear approximation of the ACOPF in terms of the real and imaginary voltage components. However, the study omits numerous physical constraints (e.g., voltage magnitudes, reactive power, and line limits). Mohapatra *et al.* [28] formulate the ACOPF in terms of incremental variables and solve the nonlinear formulation by applying Newton's and the primal-dual interior point methods but without line limits. Coffrin *et al.* [29] apply piecewise linear approximations of the cosine term and Taylor series expansions of the remaining nonlinear terms. All three studies report on limited sized networks.

There is growing interest in applying convexification techniques to the ACOPF. Like linear and quadratic programs, semidefinite programming (SDP) and second-order conic programming (SOCP) approaches can be solved in polynomial time by interior point methods. Such convex relaxations can be valuable in determining bounds on problems that are nonconvex and also to initialize local solution methods. Bai *et al.* [30] propose a semidefinite relaxation (SDR) for which Lavaei and Low [2] derive a rank-one sufficient condition under which the SDR is exact, i.e., a globally optimal solution is guaranteed. Lavaei and Low further prove that if the network is radial, then this sufficient condition always holds [2] and the second order conic relaxation (SOCR) is equivalent for these cases [31]; this can be attributed to the fact that the power flow solution of a radial network is unique [32]. A shortcoming of these convexifications is that there is no mechanism to recover an ACOPF feasible solution when the sufficient condition is not satisfied. Therefore Molzahn and Hiskens [33] and Josz *et al.* [34] propose moment relaxations in order to obtain tighter lower bounds. However, Lavaei *et al.* [35] show that even though a global optima is achieved, the solution may not satisfy the sufficient condition. Furthermore, there are still practical difficulties in efficiently implementing a SDR in a mixed integer approach, including the lack of an initialization method and limitations in scalability due to the number of linear algebraic iterations required during the solution process. Moreover, Lesieutre *et al.* [36] illustrate practical scenarios where the SDR fails to produce physically meaningful solutions.

There has been a number of SOCR formulations applied to the ACOPF, e.g., please see [37]–[41], which is considered a weaker relaxation in general. The computational effort per iteration to solve SOCP problems is greater than that required to solve linear and quadratic programs, but less than that required to solve a SDP problem of similar size and structure. Kocuk *et al.* propose strong SOCR formulations, which are an order of magnitude faster than standard SDR formulations but not as tight, and are also an order of magnitude slower yet more accurate than Jabr's original SOCR formulation [37]. The SOCR solutions are often inexact but with a finite optimality gap; closing the gap may require stronger bounds (which could guarantee a globally optimal outcome when exact) or a local solution method in order to achieve ACOPF feasibility. Although these approaches may be more suitable than SDR in a mixed integer approach, current drawbacks include the need to initialize from a strictly feasible primal-dual pair of solutions, and determining feasibility with respect to the integer variables on inexact solutions. Incorporating convex relaxations into more complex decision processes

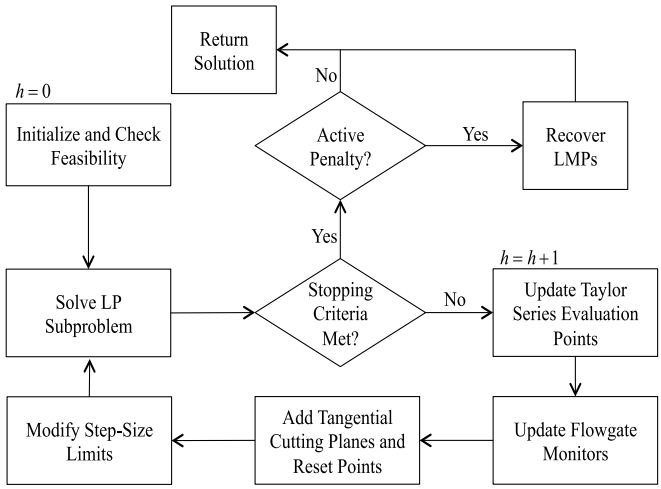

Fig. 1. The SLP IV-ACOPF Algorithm.

that also include mixed integer variables is a growing research area still in early stages of development.

In conclusion, current state-of-the-art advancements continue to demonstrate tradeoffs between convergence quality and computational performance. Given this research context, we proceed to formulate our SLP IV-ACOPF algorithm and demonstrate scalability and performance in obtaining an ACOPF optimal solution on the full range of IEEE and Polish test networks.

III. Algorithm Outline

Our overall solution strategy in the SLP IV-ACOPF is depicted in the process diagram of Fig. 1. In the initial iteration ($h = 0$), we initialize variables and the evaluation point for the first order Taylor series approximations using a flat start, warm start, or cold start. If the calculated power flows from this initialization are not feasible, we update the initializations to reside within constraint bounds. We then iteratively solve the resulting LP subproblem. Following each iteration h, we check whether the solution meets either of the following stopping criteria: (1) the solution is ACOPF feasible within a specified power mismatch tolerance or (2) a maximum iteration limit is reached (see Appendix C). If neither of these criteria are met, we update the Taylor series evaluation points, which are denoted by placing a caret or "hat" over the corresponding parameter; for an arbitrary evaluation point $\hat{x}^{(h)}$, we have that $\hat{x}^{(h)} = x^*$, which is the optimal solution from iteration $h-1$.

After updating the evaluation points, we update all flowgate monitors in order to identify lines that are near or at capacities. For any evaluation point that is ACOPF infeasible according to the nodal voltage magnitude limits and the flowgate monitors, we reset these evaluation points to be within the original bounds; accordingly, we add a tangential cutting plane for each infeasibility in order to enforce ACOPF feasibility in the following iteration. The step size bounds are also modified before re-solving the LP subproblem; these bounds limit the approximation error and control oscillations in the first order Taylor series. We impose constraint satisfaction of the inequality constraints by introducing slack variables that are penalized in the cost function.

Upon termination, the algorithm can yield one of the four following outcomes: (1) a KKT optimal solution to the ACOPF is identified, (2) the SLP solution is ACOPF feasible but not optimal, (3) the SLP solution is ACOPF infeasible, or (4) the SLP solution is infeasible. Results meeting criteria (1) through (3) may be meaningful in practice. An additional step to recover the non-penalized LMPs is required if the criteria (3) is met; to recover the LMPs, we reset all the penalty factors to equal zero and re-solve the LP subproblem where the step-size limit is set to an infinitesimal quantity. An outcome of (4) indicates that either the SLP IV-ACOPF requires a better initialization, the step size used is too small, or that the ACOPF is unbounded or has no solution.

We define a converged solution as one meeting the mismatch tolerances as set in the stopping criteria. Since the necessary optimality conditions are related to the Taylor series approximations through first order derivatives, and first order Taylor series approximations are applied to all the nonlinear terms in the formulation, we are guaranteed a KKT optimal solution within the specified tolerances when the SLP algorithm converges with no active penalties, i.e., outcome (1). For a converged solution with active penalties, we have outcome (3). Outcome (2) is a result of early termination and outcome (4) is due to early termination, infeasibility or unboundedness.

IV. Algorithm Details

In this section, we first present the network model in Section IV-A and the canonical problem formulation in Section IV-B. in Section IV-C, we linearize and reduce the nonlinear IV-ACOPF in order to construct the LP subproblem in Section IV-D.

A. Network Model

We assume balanced three-phase, steady-state conditions; the nomenclature is detailed before Section I. We formulate the nonlinear IV-ACOPF and the subsequent LP subproblem in rectangular coordinates for the voltage phasor $\mathbf{v}_n = v_n^r + \mathrm{j}v_n^j$ at each bus $n \in \mathcal{N}$, the current phasor $\mathbf{i}_n = i_n^r + \mathrm{j}i_n^j$ at each bus $n \in \mathcal{N}$, and the current phasor $\mathbf{i}_{k(\cdot)} = i_{k(\cdot)}^r + \mathrm{j}i_{k(\cdot)}^j$ on all network flows $k(\cdot) \in \mathcal{F}$.

Applying the π-model, we determine the series conductance G_k and series susceptance B_k as

$$G_k = \frac{R_k}{(R_k^2 + X_k^2)} \tag{1}$$

$$B_k = -\frac{X_k}{(R_k^2 + X_k^2)}. \tag{2}$$

In order to characterize the resistive losses and leakage flux (i.e., self-reactance), we model a practical transformer that is located on the bus n side as an ideal transformer with turns ratio $|\tau_{kn}|$ in series with a series admittance $Y_k = G_k + \mathrm{j}B_k$. Depending on if τ_{kn} is real or complex, the transformer is in-phase or phase-shifting. We can similarly represent a phase-shifter as $\tau_{kn} = |\tau_{kn}| e^{j\phi_{kn}}$. For the branch admittance matrix

$$\begin{bmatrix} Y_{1,1}^k & Y_{1,2}^k \\ Y_{2,1}^k & Y_{2,2}^k \end{bmatrix} = \begin{bmatrix} |\tau_{kn}|^2 \left(Y_k + Y_{kn}^{sh}\right) & -\tau_{kn}^* \tau_{km} Y_k \\ -\tau_{kn} \tau_{km}^* Y_k & |\tau_{km}|^2 \left(Y_k + Y_{km}^{sh}\right) \end{bmatrix}, \tag{3}$$

we model the complex current flows on line k as

$$\begin{bmatrix} \mathbf{i}_{k(n,m)} \\ \mathbf{i}_{k(m,n)} \end{bmatrix} = \begin{bmatrix} Y^k_{1,1} & Y^k_{1,2} \\ Y^k_{2,1} & Y^k_{2,2} \end{bmatrix} \times \begin{bmatrix} \mathbf{v}_n \\ \mathbf{v}_m \end{bmatrix}. \tag{4}$$

The above representation is for a two-winding transformer, and if $\tau_{kn} = \tau_{km} = 1$, then the equivalent π-model is of a transmission line. For an N-winding transformer, we would have a Y^k matrix of size $N \times N$ for the unified branch model. We can represent the linear relationship between the real and imaginary parts of the complex current flows $\mathbf{i}_{k(n,m)}$ and $\mathbf{i}_{k(m,n)}$, and the complex nodal voltages $\mathbf{v}_n$ and $\mathbf{v}_m$, as

$$i^r_{k(n,m)} = \mathrm{Re}\left(Y^k_{1,1}\mathbf{v}_n + Y^k_{1,2}\mathbf{v}_m\right) \tag{5}$$
$$i^j_{k(n,m)} = \mathrm{Im}\left(Y^k_{1,1}\mathbf{v}_n + Y^k_{1,2}\mathbf{v}_m\right) \tag{6}$$
$$i^r_{k(m,n)} = \mathrm{Re}\left(Y^k_{2,1}\mathbf{v}_n + Y^k_{2,2}\mathbf{v}_m\right) \tag{7}$$
$$i^j_{k(m,n)} = \mathrm{Im}\left(Y^k_{2,1}\mathbf{v}_n + Y^k_{2,2}\mathbf{v}_m\right) \tag{8}$$

for all flows $k(\cdot) \in F$. The nodal current balance for each bus $n \in \mathcal{N}$ is

$$i^r_n - \left(\sum_{k(n,\cdot)} i^r_{k(n,m)} + G^{sh}_n v^r_n - B^{sh}_n v^j_n\right) = 0 \tag{9}$$
$$i^j_n - \left(\sum_{k(n,\cdot)} i^j_{k(n,m)} + G^{sh}_n v^j_n + B^{sh}_n v^r_n\right) = 0. \tag{10}$$

B. IV-ACOPF Formulation

We formulate the nonlinear IV-ACOPF in rectangular coordinates where we balance on the above network current flows. Instead of introducing the square root $\left(\sqrt{\cdot}\right)$ operator, we compute the squared voltage magnitude $(v_n)^2 = (v^r_n)^2 + (v^j_n)^2$ for all buses $n \in \mathcal{N}$ and the squared current magnitude $(i_{k(\cdot)})^2 = (i^r_{k(\cdot)})^2 + (i^j_{k(\cdot)})^2$ for all flows $k(\cdot) \in \mathcal{F}$. The canonical formulation is

$$\min \sum_{n\in\mathcal{N}} C^{g,2}_n \left(p^g_n\right)^2 + C^{g,1}_n p^g_n \tag{11}$$

subject to

$$(5) - (10) \tag{12}$$
$$p^g_n - \left(v^r_n i^r_n + v^j_n i^j_n\right) = P^d_n \tag{13}$$
$$q^g_n - \left(v^j_n i^r_n - v^r_n i^j_n\right) = Q^d_n \tag{14}$$
$$P^{\min}_n \le p^g_n \le P^{\max}_n \tag{15}$$
$$Q^{\min}_n \le q^g_n \le Q^{\max}_n \tag{16}$$
$$\left(V^{\min}_n\right)^2 \le (v_n)^2 \le (V^{\max}_n)^2 \tag{17}$$
$$\left(i_{k(\cdot)}\right)^2 \le (I^{\max}_k)^2 \tag{18}$$

for all $n \in \mathcal{N}$ in (13)–(17) and all $k(\cdot) \in \mathcal{F}$ in (18). The generator offers curves in the objective function (11) are convex quadratic; this is a convex piecewise linear function in practice. The upper bounds in (17) and (18) are nonlinear and convex; (13), (14), and the lower bound in (17) are nonlinear and nonconvex. The LMP is derived from the dual variable to (13).

C. Linearization and Reduction Methods

We apply approximations, relaxations, penalty variables, and constraint set reduction in order to reformulate the nonlinearities in (11)–(18).

1) Piecewise Linear Interpolations: A piecewise linear interpolation can be applied to approximate the quadratic generator offer curve in (11) where the generators offer at marginal cost. Typically, generator offer curves are monotonically increasing, and by partitioning the interval into more linear segments, this approach results in a tighter upper bound on the quadratic cost function. In practice, generators typically offer into the market where its supply offer is a step function.

To construct the piecewise linear function, we partition the interval $\left[P^{\min}_n, P^{\max}_n\right]$ into $|\mathcal{L}|$ linear segments with length $P^g_n = \left(P^{\max}_n - P^{\min}_n\right)/|\mathcal{L}|$. There are $|\mathcal{L}|+1$ points where the l-th segment is associated with points

$$[x_l, x_{l+1}] := \left[P^{\min}_n + lP^g_n, P^{\min}_n + (l+1)P^g_n\right]. \tag{19}$$

For $l = 0, \ldots, |\mathcal{L}|$, we have that $x_0 < x_1 < \cdots < x_{|\mathcal{L}|+1}$.

For each segment $l \in \mathcal{L}$ and bus $n \in \mathcal{N}$, we calculate the midpoint and applying the slope of the offer curve in order to determine the resulting cost coefficient

$$C^g_{n,l} = C^{g,1}_n + \left(B^{\mathrm{MVA}}\right)^2 C^{g,2}_n (x_l + x_{l+1}). \tag{20}$$

Note that the $\left(B^{\mathrm{MVA}}\right)^2$ accounts for any per-unit scaling of the power variables. We approximate the aggregate offer curve in (11) as

$$\text{offers}(\cdot)^{(h)} = \sum_{n\in\mathcal{N}} \sum_{l\in\mathcal{L}} C^g_{n,l} p^g_{n,l} + C^0_n \tag{21}$$

for iteration h, where $C^0_n = C^{g,2}_n \left(P^{\min}_n\right)^2 + C^{g,1}_n P^{\min}_n$ when $P^{\min}_n > 0$.

Furthermore, each segment $p^g_{n,l}$ of the piecewise linear function is limited by P^g_n, that is

$$p^g_{n,l} \le P^g_n \tag{22}$$

for all $n \in \mathcal{N}$ and $l \in \mathcal{L}$. The aggregate of the segments at bus n must equal the real power generation

$$p^g_n = \sum_{l\in\mathcal{L}} p^g_{n,l} + P^{\min}_n \tag{23}$$

for all $n \in \mathcal{N}$.

2) Taylor Series Approximations: We apply first order Taylor series approximations to address the nonlinear terms $p^g_n, q^g_n, (v_n)^2$ and $(i_{k(\cdot)})^2$ in constraints (13), (14), (17) and (18), respectively. For iteration h, we use the Taylor series evaluation points (denoted with a caret or "hat") to approximate the first order linearizations

$$v^{sq}_n = 2\hat{v}^{r(h)}_n v^r_n + 2\hat{v}^{j(h)}_n v^j_n - \left(\hat{v}^{r(h)}_n\right)^2 - \left(\hat{v}^{j(h)}_n\right)^2 \tag{24}$$
$$p^g_n = \hat{v}^{r(h)}_n i^r_n + \hat{v}^{j(h)}_n i^j_n + v^r_n \hat{i}^{r(h)}_n + v^j_n \hat{i}^{j(h)}_n - \hat{v}^{r(h)}_n \hat{i}^{r(h)}_n - \hat{v}^{j(h)}_n \hat{i}^{j(h)}_n + P^d_n \tag{25}$$
$$q^g_n = \hat{v}^{j(h)}_n i^r_n - \hat{v}^{r(h)}_n i^j_n + v^j_n \hat{i}^{r(h)}_n - v^r_n \hat{i}^{j(h)}_n - \hat{v}^{j(h)}_n \hat{i}^{r(h)}_n + \hat{v}^{r(h)}_n \hat{i}^{j(h)}_n + Q^d_n \tag{26}$$

for all buses $\forall n \in \mathcal{N}$, and

$$i^{sq}_{k(\cdot)} = 2\hat{i}^{r(h)}_{k(\cdot)} i^r_{k(\cdot)} + 2\hat{i}^{j(h)}_{k(\cdot)} i^j_{k(\cdot)} - \left(\hat{i}^{r(h)}_{k(\cdot)}\right)^2 - \left(\hat{i}^{j(h)}_{k(\cdot)}\right)^2 \tag{27}$$

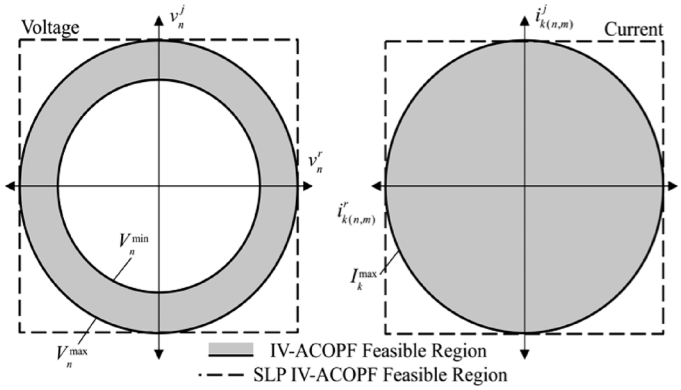

Fig. 2. Outer approximation of the voltage and current phasor bounds with box constraints.

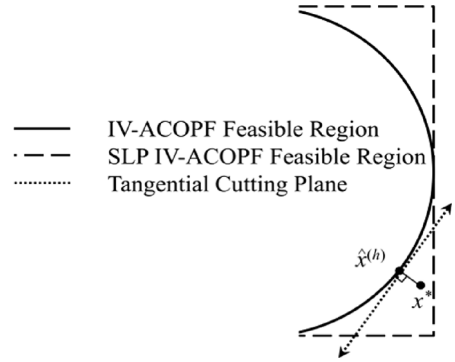

Fig. 3. The infeasible solution x^* from iteration $h-1$, the updated evaluation point $\hat{x}^{(h)}$, and the tangential cutting plane included to the constraint set for iteration h.

for all flows $\forall k(\cdot) \in \mathcal{F}$. Since a first order method is used, larger step sizes result in larger approximation error. Therefore, we must require step sizes that are small enough to gain higher accuracy (i.e., lower truncation error) but large enough to minimize the required number of iterations. Depending on the penalty and real power mismatch costs, the step size is restricted at an accelerated or decelerated rate; see Appendix A. At each iteration h, we update the tunable parameter $V_n^{(h)}$ and introduce the step size limits

$$\left|v_n^r - \hat{v}_n^{r(h)}\right| \le V_n^{(h)} \tag{28}$$

$$\left|v_n^j - \hat{v}_n^{j(h)}\right| \le V_n^{(h)} \tag{29}$$

on the real and imaginary parts of the nodal voltage, v_n^r and v_n^j, for all buses $n \in \mathcal{N}$. By controlling the step size for the real and imaginary parts of the nodal voltages, we limit the approximation error in the real and reactive power, and the corresponding error in LMP as derived from the dual variable to (25).

3) Relaxations and Penalty Factors: In conjunction with (24), we introduce the following box constraints on the real and imaginary parts of the nodal voltage as

$$-V_n^{\max} \le v_n^r \le V_n^{\max} \tag{30}$$

$$-V_n^{\max} \le v_n^j \le V_n^{\max} \tag{31}$$

for all buses $\forall n \in \mathcal{N}$, and in conjunction with (27) we introduce

$$-I_k^{\max} \le i_{k(\cdot)}^r \le I_k^{\max} \tag{32}$$

$$-I_k^{\max} \le i_{k(\cdot)}^j \le I_k^{\max} \tag{33}$$

on the real and imaginary parts for all current flows $\forall k(\cdot) \in \mathcal{F}$. These relaxed constraints bound our approximation, as illustrated in Fig. 2.

However, this approach can result in IV-ACOPF infeasible solutions. When infeasibility occurs due to violations of the voltage (17) or current (18) upper bound, we reset the violating evaluation points of the Taylor series approximation to be within these bounds. We also include a tangential cutting plane to the constraint set for the subsequent iteration, as illustrated in Fig. 3. We impose constraint satisfaction of the tangential cutting plane by introducing a slack variable, which is penalized in the cost function; see Appendix B. This approach only applies for the outer approximation on the upper bounds.

When the lower bound constraint in (17) is violated, we do not introduce a tangential cutting plane, which would eliminate parts of the IV-ACOPF feasible region. Instead, we only impose constraint satisfaction by introducing slack variables that are penalized in the cost function. We treat the bounds on the first order Taylor approximations similarly. As a result we reformulate (15)–(18) as

$$P_n^{\min} - p_n^{viol,-} \le p_n^g \le P_n^{\max} + p_n^{viol,+} \tag{34}$$

$$Q_n^{\min} - q_n^{viol,-} \le q_n^g \le Q_n^{\max} + q_n^{viol,+} \tag{35}$$

$$\left(V_n^{\min}\right)^2 - v_n^{viol,-} \le v_n^{sq} \le \left(V_n^{\max}\right)^2 + v_n^{viol,+} \tag{36}$$

$$i_{k(\cdot)}^{sq} \le \left(I_k^{\max}\right)^2 + i_{k(\cdot)}^{viol,+} \tag{37}$$

where the slack variables $p_n^{viol,+}, q_n^{viol,+}, v_n^{viol,-}, v_n^{viol,+}$, and $i_{k(\cdot)}^{viol,+}$ are penalized in the objective function.

4) Constraint Reduction: We apply the concept of flowgate monitors to solve the linearized formulation with a reduced constraint set. We compute and monitor the flows for a subset of lines $k' \in \mathcal{K}'^{(h)} \subset \mathcal{K}$ where $k'(\cdot) \in \mathcal{F}$ are near or at $(I_{k'}^{\max})^2$. The subset of lines $\mathcal{K}'^{(h)} \subset \mathcal{K}$ is updated at each iteration $h > 0$. The constraint set is therefore reduced to only include (27), (32), (33), and (37) for all $k(\cdot) = k(\cdot)' \in \mathcal{F}$.

D. LP Subproblem Formulation

For each iteration h, the SLP IV-ACOPF solves the following LP subproblem:

$$\text{cost}(\cdot)^{(h)} = \min\Big(\text{offers}(\cdot)^{(h)} + \text{penalty}(\cdot)^{(h)}\Big) \tag{38}$$

subject to

$$(5)-(10), (22)-(37), \text{ Appendix VIII-B line } (4) \tag{39}$$

where $\text{offers}(\cdot)^{(h)}$ is defined in (21) and $\text{penalty}(\cdot)^{(h)}$ is defined as

$$\begin{aligned}\text{penalty}(\cdot)^{(h)} &= \sum_{n\in\mathcal{N}}\Big[P_n^{\epsilon}\left(p_n^{viol,-} + p_n^{viol,+}\right) \\ &\quad + Q_n^{\epsilon}\left(q_n^{viol,-} + q_n^{viol,+}\right) + V_n^{\epsilon}\left(v_n^{viol,-} + v_n^{viol,+}\right)\Big] \\ &\quad + \sum_{k'\in\mathcal{K}'^{(h)}} I_{k'}^{\epsilon}\left(i_{k'(n,m)}^{viol,+} + i_{k'(m,n)}^{viol,+}\right).\end{aligned} \tag{40}$$

The tangential cutting planes in line (4) of the process in Appendix B are included in order to modify any IV-ACOPF infeasibilities from the prior solution, for iterations $h > 0$.

V. Results

We now test the computational performance and convergence quality of the SLP IV-ACOPF and compare the results to solving the nonlinear IV-ACOPF as defined by the piecewise linear cost function in (21) and constraint set in (12)–(18), (22) and (23). In [23] we demonstrate that the mathematical formulation, solver algorithm, and initialization all contribute to the performance of ACOPF solution techniques. Therefore we focus on the mathematical formulations proposed in this work, and compare performance of the SLP versus NLP approaches for various solvers and initializations.

For the nonlinear IV-ACOPF, we are unable to obtain globally optimal rank-one solutions from a semidefinite relaxation without augmenting the formulation to include penalties on constraint violations, and in many cases these penalties were non-uniform and thus difficult to non-arbitrarily determine a global optimum. Instead, we report an upper bound on solution cost by solving the IV-ACOPF with KNITRO MS (multi-start) using the default settings[42], which we refer to as NLP/KNITRO MS. Although a global optimum is not guaranteed, the probability of finding a better local solution is higher with multi-start on the globally convergent KNITRO algorithms (Interior/CG, Interior/Direct, Active-Set). Since the KNITRO multi-start runtime is much longer than that of our SLP IV-ACOPF algorithm, the CPU time reported is for KNITRO without multi-start. We also solve the nonlinear IV-ACOPF with IPOPT, which uses a filter line search to ensure global convergence [43].

Both the IV-ACOPF model and SLP IV-ACOPF algorithm are implemented in Python 2.7 with Pyomo 3.5 [44] and executed on a workstation with four quad-core Intel Xeon 2.7 GHz processors with hyper-threading and 512 GB RAM. We solve the LP subproblems of the SLP IV-ACOPF with either Gurobi 5.6.2 [45] or CPLEX 12.5.1 [46] barrier method limited to two threads, and the IV-ACOPF with either IPOPT 3.11.4 configured using the MA27 linear sub-solver (no multi-threading support) [43] or KNITRO 9.1, where KNITRO chooses the algorithm to apply [42]; we refer to each set of simulations as SLP/Gurobi, SLP/CPLEX, NLP/IPOPT, and NLP/KNITRO, respectively. Since MATPOWER 5.1 [47] specifically formulates the ACOPF in polar coordinates and augments user-specified initializations by selecting an interior point, we were unable to readily include the MATPOWER 5.1 solvers into our testing. A feasibility and optimality tolerance of $1.0\mathrm{E}-06$ is applied to each solver in our study.

We execute each algorithm from multiple starting points on a publicly available test suite consisting of: (1) IEEE networks 14, 30, 57, 118, 300, and (2) Polish networks 2383 wp, 2737 sop, 2746 wop, 3012 wp, 3120 sp, 3375 wp, where the number represents the number of buses in the respective network model, and the acronyms are "sp" for summer peak, "sop" for summer off-peak, "wp" for winter peak, and "wop" for winter off-peak [47]. For buses with multiple generators, we aggregate these units with an average cost function. We solve these networks without line limits for a baseline case and with line limits (not including network elements) for a thermally constrained case. We use the approach by Lipka *et al.* [48] to systematically compute line ratings in terms of current, as presented in Table II.

TABLE I
PARAMETER DEFAULTS. NOTE THAT THE FLAT START REQUIRES A SLOWER RATE a IN STEP-SIZE DECREASE DUE TO POOR INITIAL START QUALITY

Parameter	Description	Value
LIM	Iteration Limit	20
$\lvert\mathcal{L}\rvert$	Piecewise Segments	10
a	Step-Size Parameter	0.25
b	Step-Size Parameter	1.5
$r^2\left(I_k^{max}\right)^2$	Flowgate Monitor Rate	$r = 0.9$
$I_{k'}^{\epsilon}$	Line Current Penalty	$25\max_n C_n^{g,1}$
V_n^{ϵ}	Voltage Penalty	$15\max_n C_n^{g,1}$
Q_n^{ϵ}	Reactive Power Penalty	$12.5\max_n C_n^{g,1}$
P_n^{ϵ}	Real Power Penalty	$2.5\max_n C_n^{g,1}$
Δ_n^{P-tol}	P-Mismatch Tolerance	1.0E−3
Δ_n^{Q-tol}	Q-Mismatch Tolerance	5.0E−3
Δ^{P-tol}	Total P-Mismatch Tolerance	$5\Delta_n^{P-tol}$
Δ^{Q-tol}	Total Q-Mismatch Tolerance	$10\Delta_n^{Q-tol}$

TABLE II
THERMAL LINE LIMITS IN TERMS OF CURRENT (MVA) AT 1 P.U. VOLTAGE

Network	Line Limits (MVA)
IEEE-14	26.75
IEEE-30	31.25
IEEE-57	142.75
IEEE-118	114
IEEE-300	682
Polish Networks	$S_{k(\cdot)}^{max} / \min_{i=n,m\in k(\cdot)} V_i^{max} \quad \forall k \in \mathcal{K}$

The performance of any SLP-based algorithm is highly dependent on strategies used, the computer implementation, and parameter settings [49]. In the proposed SLP algorithm, there are parameters to control penalty factors, constraint reduction, iterative step-size, and power mismatch tolerances. It is impossible to fine-tune these parameters to have optimal settings for all possible problems without skewing the results, so we demonstrate performance for the default values as reported in Table I. The magnitude of the penalties, on average, are loosely correlated to the types of constraint most likely to incorporate slack into the solution. For example, the penalty on the real power is the lowest since dispatching it is already priced into the market. The iteration limit was arbitrarily set to 20 for the reported test suite, but it could be set higher for larger scale or more constrained networks that might require more iterations. The step-size parameters a and b tune the parameters α and β as described in Appendix A. Most importantly, a controls the rate of decay in the allowable step-size, where the default step-size region varies in proportion to the power of the iteration count, as determined by b when there are excessive penalties present. We apply power mismatch tolerances well below the threshold of known state estimator precision; in practice and as we demonstrate below, high accuracy in convergence is not required to obtain a meaningful result.

We consider four types of initialization methods: (1) flat start, (2) DC warm start, (3) AC warm start, and (4) uniform cold start. The flat start assumes unit voltage and half-max output for all generation. The DC and AC warm starts are constructed from DCOPF and ACOPF locally optimal solutions,

TABLE III
THE SCALING FACTOR p FOR THE EXPERIMENTAL TIME COMPLEXITY, $\Theta\left(n^p\right)$, WITH CORRESPONDING R-SQUARED (R^2) AND ROOT MEAN SQUARED ERROR (RMSE) VALUES, OF NLP/KNITRO, NLP/IPOPT, SLP/CPLEX, AND SLP/GUROBI. THE EXPONENT $p = 1$ CORRESPONDS TO LINEAR ALGORITHMIC SCALING. THE HIGH R-SQUARED VALUES INDICATE THAT THE TIME COMPLEXITY MODEL n^p EXPLAINS NEARLY ALL THE VARIABILITY IN COMPUTATIONAL TIME AS A FUNCTION OF THE NETWORK SIZE. RMSE IS REPORTED IN SECONDS (s); A VALUE CLOSER TO ZERO INDICATES A FIT THAT IS MORE USEFUL FOR PREDICTION

		Best-Case Simulations			All Converged Simulations		
		p	R^2	RMSE (s)	p	R^2	RMSE (s)
Baseline Cases	NLP/KNITRO	1.42	0.83	1.46	1.47	0.82	1.40
	NLP/IPOPT	1.13	0.95	0.60	1.34	0.97	0.50
	SLP/CPLEX	0.97	0.99	0.20	1.01	0.98	0.33
	SLP/Gurobi	1.01	0.99	0.21	1.03	0.98	0.33
Thermally Constrained Cases	NLP/KNITRO	1.39	0.88	1.13	1.39	0.89	1.08
	NLP/IPOPT	1.11	0.98	0.36	1.22	0.97	0.50
	SLP/CPLEX	0.99	0.99	0.17	1.00	0.98	0.31
	SLP/Gurobi	1.06	0.99	0.23	1.05	0.97	0.36

TABLE IV
THE FASTEST RECORDED SOLVER CPU TIME ACROSS ALL SIMULATIONS FOR BOTH BASELINE AND THERMALLY CONSTRAINED NETWORKS. THE NUMBER OF SLP SUBPROBLEM ITERATIONS IS DENOTED IN PARENTHESES

Solver CPU Time	Baseline Case				Thermally Constrained Case			
(s)	NLP/Knitro	NLP/IPOPT	SLP/CPLEX	SLP/Gurobi	NLP/Knitro	NLP/IPOPT	SLP/CPLEX	SLP/Gurobi
IEEE-14	0.12	0.16	0.24 (4)	0.25 (4)	0.12	0.19	0.19 (3)	0.17 (3)
IEEE-30	0.19	0.2	0.84 (9)	0.89 (9)	0.19	0.19	0.58 (6)	0.67 (6)
IEEE-57	0.32	0.38	0.76 (5)	0.95 (5)	0.32	0.35	0.79 (5)	1.03 (5)
IEEE-118	0.84	1.18	2.53 (7)	3.49 (7)	1.23	1.18	2.86 (7)	3.49 (7)
IEEE-300	2.27	2.63	4.88 (6)	9.23 (6)	1.96	2.22	5.23 (6)	8.86 (6)
Polish-2,383	38.65	88.47	37.05 (6)	68.62 (6)	43.63	26.32	36.42 (6)	64.27 (6)
Polish-2,737	29.57	25.29	42.69 (6)	58.63 (6)	31.29	46.37	41.79 (6)	54.69 (6)
Polish-2,746	42.43	20.67	51.71 (7)	70.62 (7)	82.02	39.66	43.78 (6)	68.34 (6)
Polish-3,012	96.51	33.15	49.73 (6)	68.22 (6)	99.53	35.56	46.34 (6)	68.69 (6)
Polish-3,120	84.34	30.47	57.17 (6)	70.55 (6)	66.46	31.22	49.54 (6)	75.73 (6)
Polish-3,375	6,473.40	145.05	59.39 (6)	83.97 (6)	2,348.57	80.51	61.95 (6)	89.28 (6)

respectively, where the demand is parameterized as $P_n^d \sim \mathcal{U}\left(0.9P_n^d, 1.1P_n^d\right)$ for all $n \in \mathcal{N}$. The uniform starts assume that $v_n^r \sim \mathcal{U}\left(V_n^{\min}, V_n^{\max}\right)$ and $v_n^j = 0$ for all $n \in \mathcal{N}$; given that the uniform start does not incorporate any knowledge of a prior operating state, it is by definition a cold start. The sample size for the various initialization types is one sample for the flat start and 10 samples for the remaining start types. To reduce variance in the comparison, we use identical starting points to test SLP/Gurobi, SLP/CPLEX, NLP/IPOPT, and NLP/KNITRO.

The overall frequency of convergence is as follows. For the nonlinear IV-ACOPF, NLP/KNITRO and NLP/IPOPT converged 99.7% and 96.9% of the time, respectively. For the SLP algorithms we define a converged solution as meeting the mismatch tolerances defined in Table I as set in the stopping criteria; see Appendix C and Section III for implementation details. For LP subproblem iterations that are locally infeasible or if the iteration count reaches the user defined limit, then the simulation is labeled as unconverged. SLP/CPLEX converged in 98.4% of the runs and the SLP/Gurobi in 99.1% of the runs. Of the converged runs, 10.3% of the SLP/CPLEX and 10.3% of the SLP/Gurobi runs resulted in active penalties; these only occurred in the IEEE-118 and Polish-2,383 thermally constrained cases. The active penalty in the thermally constrained IEEE-118 is due to reactive power compensation requirements at a single bus located in a congested area of the network. The active penalty in the Polish-2,383 is on a real power injection at a single generator bus; by increasing the real power penalty by a factor of three so that $P_n^{\epsilon} = 7.5 \max_n C_n^{g,1}$, SLP/CPLEX and SLP/Gurobi converge to the unpenalized optimum. As is evident, the SLP parameterization ideally should be determined on a case-by-case basis, but for the purpose of demonstrating general application and performance, we apply default parameters here.

TABLE V
OFFER PRODUCTION COSTS FOR THE BEST-KNOWN MULTI-START SOLUTIONS FOUND BY NLP/KNITRO MS

Offer Production Cost ($)	Baseline Case NLP/Knitro MS	Thermally Constrained Case NLP/Knitro MS
IEEE-14	8,091	9,294
IEEE-30	575	582
IEEE-57	41,817	41,978
IEEE-118	129,903	135,189
IEEE-300	720,149	726,794
Polish-2,383	1,858,447	1,863,627
Polish-2,737	742,679	742,688
Polish-2,746	1,185,115	1,185,507
Polish-3,012	2,581,020	2,597,386
Polish-3,120	2,137,309	2,140,727
Polish-3,375	7,402,883	7,415,108

To analyze algorithm scaling properties, we determine the experimental time complexity $\Theta\left(T\left(n\right)\right)$ classified by the nature of the function $T\left(n\right) = n^p$ for network size n and unknown exponent $p > 0$. Instead of reporting numerous run time samples, Big-Theta ("Θ") reports the exact dependence of the run time on network size for the subset of converged simulations in this study. We apply a linear regression on $\log\left(s\right) = p\log\left(n\right) + \log\left(b\right)$ to determine the power function $s = bn^p$, where s is the simulation run time and the coefficient b (relating to the y-intercept of $\log\left(b\right)$) is irrelevant when determining the order of $T\left(n\right)$. We use the MATLAB function polyfit , which minimizes the sum of the squares of the data deviations from the least-squares fit [50]. In Table III, we report the experimental

TABLE VI
THE RELATIVE CONVERGENCE QUALITY IN THE OPTIMAL SOLUTION, AS COMPARED TO THE BEST-KNOWN MULTI-START SOLUTION IN TABLE V, FOR THE FASTEST RECORDED RUN AS PRESENTED IN TABLE IV; A POSITIVE (NEGATIVE) METRIC INDICATES THE RELATIVE INCREASE (DECREASE) AMOUNT IN SOLUTION VALUE. BY DECREASING THE MISMATCH TOLERANCE IN THE SLP ALGORITHM, AS DEFINED IN TABLE I, WE CAN EFFECTIVELY DECREASE THE RELATIVE CHANGE IN EXCHANGE FOR MORE COMPUTATIONAL TIME

Relative Change	Baseline Case				Thermally Constrained Case			
to Table V Solution	NLP/Knitro	NLP/IPOPT	SLP/CPLEX	SLP/Gurobi	NLP/Knitro	NLP/IPOPT	SLP/CPLEX	SLP/Gurobi
IEEE-14	0.0E+00	0.0E+00	1.2E-04	1.2E-04	0.0E+00	0.0E+00	-3.2E-04	-3.2E-04
IEEE-30	0.0E+00	0.0E+00	0.0E+00	0.0E+00	0.0E+00	0.0E+00	1.7E-02	2.4E-02
IEEE-57	0.0E+00	0.0E+00	5.3E-04	1.7E-04	0.0E+00	0.0E+00	2.4E-04	-4.8E-05
IEEE-118	0.0E+00	0.0E+00	1.2E-03	1.2E-03	0.0E+00	0.0E+00	3.0E-03	5.1E-03
IEEE-300	0.0E+00	0.0E+00	3.6E-05	1.9E-05	0.0E+00	0.0E+00	2.3E-05	2.2E-05
Polish-2,383	0.0E+00	0.0E+00	2.6E-04	4.8E-04	0.0E+00	0.0E+00	-1.4E-03	-1.8E-03
Polish-2,737	0.0E+00	0.0E+00	1.1E-04	1.1E-04	0.0E+00	0.0E+00	7.3E-05	5.1E-05
Polish-2,746	0.0E+00	0.0E+00	1.8E-04	1.8E-04	0.0E+00	0.0E+00	2.4E-04	2.3E-04
Polish-3,012	0.0E+00	0.0E+00	1.4E-04	3.7E-04	0.0E+00	0.0E+00	4.7E-04	4.1E-04
Polish-3,120	0.0E+00	0.0E+00	2.0E-04	1.4E-04	0.0E+00	0.0E+00	3.2E-04	3.0E-04
Polish-3,375	5.4E-07	2.7E-07	1.2E-03	1.4E-03	2.1E-07	1.5E-07	1.3E-03	1.3E-03

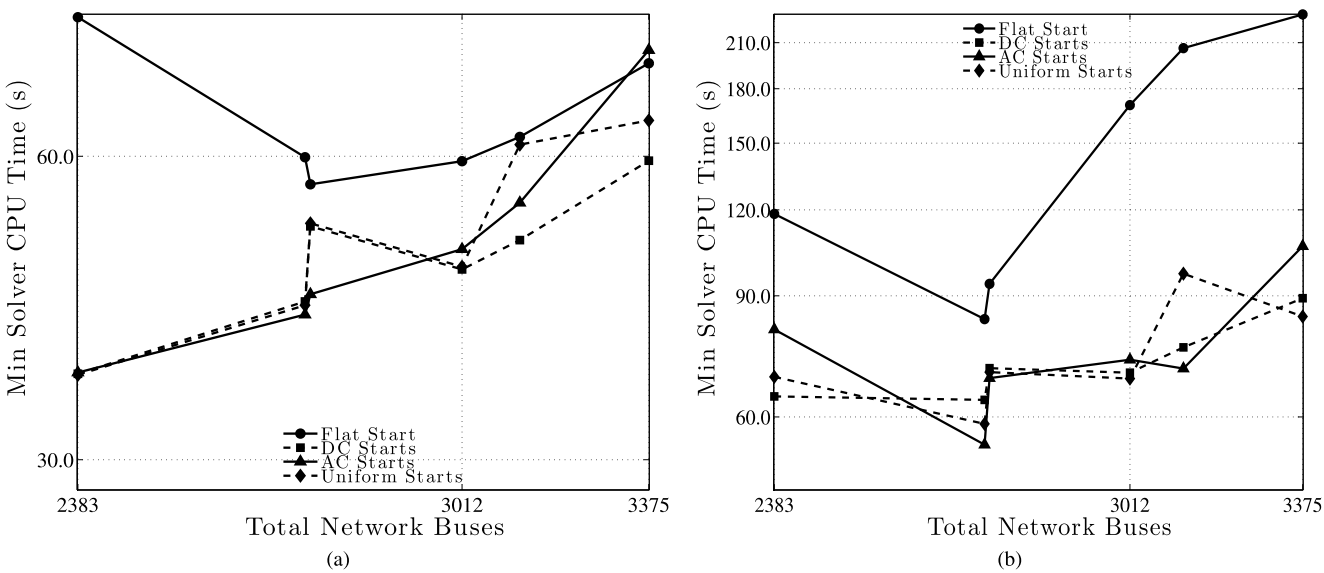

Fig. 4. The fastest recorded CPU time for SLP/CPLEX in (a) and SLP/Gurobi in (b) on each initialization type in both the baseline and thermally constrained Polish networks.

best-case and overall (i.e., for all the converged runs) time complexity exponent, along with the corresponding R-squared and root mean squared error (RMSE) values. The high R-squared values and low RMSE values (for NLP/IPOPT, SLP/CPLEX, and SLP/Gurobi) indicate the potential for IV-ACOPF and our SLP IV-ACOPF algorithm in practical applications. For p near 1 (linear), the running time of the SLP algorithm grows *nearly* directly proportional to the network size n.

The time complexity across all the simulations, as reported in the right panel of Table III, is figuratively comparable to that of the best-case, as reported in the left panel. The best-case corresponds to the fastest recorded solver CPU time for each test configuration; the run times for these simulations are reported in Table IV, and the number of SLP subproblem iterations (where applicable) are reported in parentheses. The best-case is of particular interest as the SLP/Gurobi, SLP/CPLEX, NLP/IPOPT, and NLP/KNITRO approaches can be run in parallel from various starting points. In Table V, we report the offer production costs associated with the best-known multi-start solutions, i.e., offers $(\cdot)^{(h)}$ in (38), as determined by NLP/Knitro MS (multi-start). In Table VI, we report how the best-case solutions from the various algorithmic approaches compare to the multi-start solution. The results indicate that the SLP algorithm solutions are extremely close in quality to the multi-start solutions, representing a small fraction of a single cost unit in problems where overall costs range from hundreds to millions of units. By decreasing the mismatch tolerance and any active penalties-if present-in the SLP algorithm, we can effectively decrease the relative change in exchange for more computational time. Since NLP/KNITRO and NLP/IPOPT do no worse than the NLP/KNITRO MS, this indicates that the best-known optimum is most likely the only optimum found.

In Fig. 4(a) and (b), we report the fastest recorded solve times across the four initialization types for SLP/CPLEX and SLP/Gurobi, aggregating on both the baseline and thermally constrained cases. The flat start does not perform competitively for the IV-ACOPF formulation. With the flat start ($v_n^r = 1$ and $v_n^j = 0$ for all $n \in \mathcal{N}$), the current flows are initialized to zero across symmetric transmission elements, and the Taylor series approximations in (24)–(26) are such that the entire first order expansion is not assessed for the initial iteration $h = 0$. However, the uniform starts perform competitively compared

to the DCOPF and ACOPF starts. The uniform starts do not require any knowledge of the prior operating state; by initializing v_n^r with some variation, in polar coordinates the voltage magnitudes become nonzero while the voltage angles remain zero. In the initial iteration, the current flows are nonzero; as a result, the nodal real power injections are calculated in terms of the network conductance and the nodal reactive power injections in terms of the network susceptance.

VI. Discussion

We formulate the IV-ACOPF, which has a linear network representation where nonconvex constraints are isolated to each bus, and propose an SLP-based approach to solve the problem. We demonstrate acceptable quality of convergence to best-known solutions and linear scaling of computational time in proportion to network size when leveraging commercial LP solvers. The proposed approach has flexibility in balancing the trade-offs between optimality and tractability and can be integrated into more complex models (e.g., including integer variables) that include discrete controls or system states in order to represent decision-making processes in both the operational and planning levels, while still leveraging commercial solver performance. Unlike well-established methods of approximation, such as the DCOPF with loss factor modeling and AC feasibility, the SLP IV-ACOPF co-optimizes real and reactive power dispatch and enables the system operator more optimal control over system resources.

Current limitations of the proposed work is that for nonconvex problems, there is no known theoretical convergence results to the global optimum for SLP algorithms. Fletcher *et al.* prove global convergence (i.e., convergence to a stationary point from an arbitrary initialization point) for SLP with a filter method to solve NLP problems that contain just inequality constraints [51]. Also, given that the second order information is constant in the IV-ACOPF formulation, utilizing constant Hessian matrices can increase the efficiency of each iteration in the solution technique.

In future work, we plan to integrate the SLP algorithm in more complex models to include decision-making processes and to model controllable network elements, such as FACTS devices. In terms of algorithm development, we plan to explore filter methods that avoid the pitfalls of the current penalty function approach to enforce more robust performance from any initialization.

Appendix
Supporting Details

A. Step-Size Limits

At the end of each iteration $h > 0$, we modify the tunable parameter $V_n^{(h)}$ to control the approximation error. As the approximation nears ACOPF feasibility, we accelerate the convergence rate; if the approximation worsens, we decelerate this rate through calculating the ratio

$$\gamma^{(h)} = \frac{\text{penalty}\left(\cdot\right)^{(h)} + f\left(\cdot\right)^{(h)}}{\text{cost}\left(\cdot\right)^{(h)} + f\left(\cdot\right)^{(h)}} \tag{A.41}$$

where $0 \leq \gamma^{(h)} \leq 1$,

$$f\left(\cdot\right)^{(h)} = \sum_{n \in \mathcal{N}} \text{MISMATCH}_n^{\epsilon} \left| P_n^* - p_n^g \right| \tag{A.42}$$

and

$$P_n^* = P_n^d + v_n^{r*} i_n^{r*} + v_n^{j*} i_n^{j*}. \tag{A.43}$$

As $\gamma^{(h)} \to 0$, the solution becomes ACOPF feasible, i.e., $f\left(\cdot\right)^{(h)} = 0$ and penalty $\left(\cdot\right)^{(h)} = 0$. We calculate tunable parameters $\beta = -a \log \gamma^{(h)} + b$ and $\alpha = \delta/\beta$ for $\delta = 1 - \lfloor 10\gamma^{(h)} \rfloor / 10$ where the allowable step-size is

$$V_n^{(h)} \leftarrow \frac{\alpha \left| V_n^{\max} \right|}{h^{\beta}}. \tag{A.44}$$

For faster decay, the user can increase a. When $\gamma^{(h)} = 1$, then $\beta = b$.

B. Infeasibility Handling

The following routine determines the updated evaluation point and resulting tangential cutting plane when the voltage magnitude upper bound in (17) or the thermal line limit in (18) is violated by the optimal solution of the LP subproblem in iteration h. Without loss of generality, we denote the real part as x^r, the imaginary part as x^j, and the upper bound as $X^{\max}$.

if $\left(\hat{x}^{r(h)}\right)^2 + \left(\hat{x}^{j(h)}\right)^2 > \left(X^{\max}\right)^2$ **then**

$\hat{x}^{r(h)} \leftarrow \left(\hat{x}^{r(h)}\right) \sqrt{\left(X^{\max}\right)^2 \Big/ \left(\left(\hat{x}^{r(h)}\right)^2 + \left(\hat{x}^{j(h)}\right)^2\right)}$

$\hat{x}^{j(h)} \leftarrow \left(\hat{x}^{j(h)}\right) \sqrt{\left(X^{\max}\right)^2 \Big/ \left(\left(\hat{x}^{r(h)}\right)^2 + \left(\hat{x}^{j(h)}\right)^2\right)}$

add constraint: $\hat{x}^{r(h)} x^r + \hat{x}^{j(h)} x^j \leq \left(X^{\max}\right)^2 + x^{viol,+}$

end if

C. Stopping Criteria

The stopping criteria assesses three possible scenarios: (1) the mismatch error on real and reactive power injections for all buses $n \in \mathcal{N}$ is less than a specified tolerance, (2) the net of these mismatches is less than a specified tolerance, or (3) the maximum iteration limit has been reached.

$P_n^* = P_n^d + v_n^{r*} i_n^{r*} + v_n^{j*} i_n^{j*}$

$Q_n^* = Q_n^d + v_n^{j*} i_n^{r*} - v_n^{r*} i_n^{j*}$

for all $n \in N$ **do**

$\delta_n^p \leftarrow \left|P_n^* - p_n^g\right| \Big/ \min\left(\left|P_n^*\right|, \left|p_n^g\right|\right)$

$\delta_n^q \leftarrow \left|Q_n^* - q_n^g\right| \Big/ \min\left(\left|Q_n^*\right|, \left|q_n^g\right|\right)$

end for

if $\left(\begin{array}{c} \max\limits_{n \in N} \delta_n^p \leq \Delta_n^{P-tol} \textbf{ and } \max\limits_{n \in N} \delta_n^q \leq \Delta_n^{Q-tol} \\ \textbf{or } \sum_{n \in \mathcal{N}} \delta_n^p \leq \Delta^{P-tol} \textbf{ and } \sum_{n \in \mathcal{N}} \delta_n^q \leq \Delta^{Q-tol} \\ \textbf{or } h \geq \text{LIM} \end{array} \right)$ **then**

return solution;

end if

ACKNOWLEDGMENT

We acknowledge the contributions of our co-authors on the FERC "Optimal Power Flow and Formulation Papers" series. The views presented are the views of the authors and not the FERC or any of its Commissioners. We would also like to acknowledge our anonymous reviewers for their assistance in improving the quality of this manuscript.

REFERENCES

[1] J. Carpentier, "Contribution a l'etude du dispatching economique," *Bull. Soc. Francaise Elect.*, vol. 3, pp. 431–447, 1962.
[2] J. Lavaei and S. H. Low, "Zero duality gap in optimal power flow problem," *IEEE Trans. Power Syst.*, vol. 27, no. 1, pp. 92–107, Feb. 2012.
[3] B. Stott and O. Alsaç, "Optimal Power Flow: Basic Requirements for Real-Life Problems and their Solutions," Consultants, Tech. Rep., Arizona, USA, 2012.
[4] K. Purchala, L. Meeus, D. V. Dommelen, and R. Belmans, "Usefulness of DC power flow for active power flow analysis," in *Proc. IEEE Power & Energy Soc. General Meeting*, 2005.
[5] F. S. Report, Order Conditionally Accepting Tariff Revisions and Requiring Compliance Filing for Docket Nos. ER12-678-000 and ER12-679-000, 2012.
[6] "The Value of Economic Dispatch," A Report to Congress Pursuant to Section 1234 of the Energy Policy Act of 2005, Tech. Rep., United States Dept. of Energy, 2005.
[7] R. P. O'Neill, T. Dautel, and E. Krall, "Recent ISO Software Enhancements and Future Software and Modeling Plans," Tech. Rep., FERC, 2011.
[8] M. B. Cain, R. P. O'Neill, and A. Castillo, "Optimal Power Flow Papers: Paper 1. History of Optimal Power Flow and Formulations," Tech. Rep., FERC, 2013.
[9] H. Liu, L. Tesfatsion, and A. Chowdhury, "Locational marginal pricing basics for restructured wholesale power markets," in *Proc. IEEE Power & Energy Soc. General Meeting*, 2009.
[10] E. Nicholson, "Operator-Initiated Commitments in RTO and ISO Markets," Tech. Rep., FERC, 2014.
[11] A. Castillo and R. P. O'Neill, "Survey of Approaches to Solving the ACOPF," Tech. Rep., FERC, 2013.
[12] S. H. Low, "Convex relaxation of optimal power flow, Part I: Formulations and equivalence," *IEEE Trans. Control Netw. Syst.*, vol. 1, no. 1, pp. 15–27, 2014.
[13] S. Low, "Convex relaxation of optimal power flow, Part II: Exactness," *IEEE Trans. Control Netw. Syst.*, vol. 1, no. 2, pp. 177–189, 2014.
[14] M. Huneault and F. D. Galiana, "A survey of the optimal power flow literature," *IEEE Trans. Power Syst.*, vol. 6, no. 2, pp. 762–770, May 1991.
[15] J. Momoh, M. El-Hawary, and R. Adapa, "A review of selected optimal power flow literature to 1993. Part I: Nonlinear and quadratic programming approaches," *IEEE Trans. Power Syst.*, vol. 14, no. 1, pp. 96–104, Feb. 1999.
[16] J. Momoh, M. El-Hawary, and R. Adapa, "A review of selected optimal power flow literature to 1993. Part II: Newton, linear programming, and interior point methods," *IEEE Trans. Power Syst.*, vol. 14, no. 1, pp. 105–111, Feb. 1999.
[17] S. Frank, I. Steponavice, and S. Rebennack, "Optimal power flow: A bibliographic survey I," *Energy Syst.*, vol. 3, pp. 221–258, 2012.
[18] S. Frank, I. Steponavice, and S. Rebennack, "Optimal power flow: A bibliographic survey II," *Energy Syst.*, vol. 3, pp. 259–289, 2012.
[19] H. Dommel, W. Tinney, and W. Powell, "Further developments in Newton's method for power system applications," in *Proc. IEEE PES Winter Power Meeting*, 1970, vol. CP 161-PWR, no. 70.
[20] W. F. Tinney and C. Hart, "Power flow solution by Newton's method," *IEEE Trans. Power App. Syst.*, vol. PAS-93, pp. 859–869, 1974.
[21] V. D. Costa, N. Martins, and J. Pereira, "Developments in the Newton-Raphson power flow formulation based on current injections," *IEEE Trans. Power Syst.*, vol. 14, no. 4, pp. 1320–1326, Nov. 1999.
[22] W. Rosehart and J. Aguado, "Alternative optimal power flow formulations," in *Proc. 14th Power Syst. Computat. Conf. (PSCC)*, 2002.
[23] A. Castillo and R. P. O'Neill, "Computational Performance of Solution Techniques Applied to the ACOPF," Tech. Rep., FERC, 2013.
[24] O. Alsaç and B. Stott, "Decoupled algorithms in optimal load flow calculation," in *Proc. IEEE Power Eng. Soc. 1975 Summer Meeting*, 1975.
[25] D. S. Kirschen and H. P. V. Meeteren, "MW/voltage control in a linear programming based optimal power flow," *IEEE Trans. Power Syst.*, vol. 3, no. 2, pp. 481–489, May 1988.
[26] O. Alsaç, J. Bright, M. Prais, and B. Stott, "Further developments in LP-based optimal power flow," *IEEE Trans. Power Syst.*, vol. 5, no. 3, pp. 697–711, Aug. 1990.
[27] J. Franco, M. J. Rider, M. Lavorato, and R. Romero, "A set of linear equations to calculate the steady-state operation of an electrical distribution system," in *Proc. 2011 IEEE PES Conf. Innovative Smart Grid Technologies (ISGT Latin America)*, 2011, pp. 1–5.
[28] A. Mohapatra, P. Bijwe, and B. Panigrahi, "Efficient sequential nonlinear optimal power flow approach using incremental variables," *IET Gener., Transm., Distrib.*, vol. 7, no. 12, pp. 1473–1480, 2013.
[29] C. Coffrin and P. V. Hentenryck, "A Linear-Programming Approximation of AC Power Flows," Tech. Rep., Univ. Melbourne, 2013 [Online]. Available: arXiv:1206.3614v3
[30] X. Bai, H. Wei, K. Fujisawa, and Y. Wang, "Semidefinite programming for optimal power flow problems," *Int. J. Electr. Power Energy Syst.*, vol. 30, no. 6-7, pp. 383–392, 2008.
[31] S. Sojoudi and J. Lavaei, "On the exactness of semidefinite relaxation for nonlinear optimization over graphs: Part II," in *Proc. IEEE 52nd Annu. Conf. Decision and Control (CDC)*, 2013, pp. 1051–1057.
[32] D. Das, D. P. Kothari, and A. Kalam, "Simple and efficient method for load flow solution of radial distribution networks," *Elect. Power Energy Syst.*, vol. 17, no. 5, pp. 335–346, 1995.
[33] D. K. Molzahn and I. A. Hiskens, "Sparsity-exploiting moment-based relaxations of the optimal power flow problem," *IEEE Trans. Power Syst.*, vol. 30, no. 6, pp. 3168–3180, Nov. 2015.
[34] C. Josz, J. Maeght, P. Panciatici, and J. C. Gilbert, "Application of the moment-SOS approach to global optimization of the OPF problem," *IEEE Trans. Power Syst.*, vol. 30, no. 1, pp. 463–470, Jan. 2015.
[35] J. Lavaei, D. Tse, and B. Zhang, "Geometry of power flows and optimization in distribution networks," *IEEE Trans. Power Syst.*, vol. 29, no. 2, pp. 572–583, Mar. 2014.
[36] B. C. Lesieutre, D. K. Molzahn, A. R. Borden, and C. L. DeMarco, "Examining the limits of the application of semidefinite programming to power flow problems," in *Proc. 49th Annu. Allerton Conf. Communication, Control and Comput.*, 2011.
[37] R. A. Jabr, "Radial distribution load flow using conic programming," *IEEE Trans. Power Syst.*, vol. 21, no. 3, pp. 1458–1459, Aug. 2006.
[38] R. Madani, S. Sojoudi, and J. Lavaei, "Convex relaxation for optimal power flow problem: Mesh networks," in *Proc. Asilomar Conf. Signals, Systems and Computers (ACSSC)*, 2013, pp. 1375–1382.
[39] B. Kocuk, S. Dey, and X. Sun, "Inexactness of SDP Relaxation and Valid Inequalities for Optimal Power Flow," Tech. Rep., Sch. Ind. Syst. Eng., Georgia Inst. Technol., 2014.
[40] B. Kocuk, S. S. Dey, and A. Sun, "Strong SOCP Relaxations for the Optimal Power Flow Problem," Tech. Rep., Georgia Inst. Technol., 2015.
[41] C. Coffrin, H. L. Hijazi, and P. V. Hentenryck, "The QC Relaxation: Theoretical and Computational Results on Optimal Power Flow," Tech. Rep., NICTA, 2015.
[42] R. H. Byrd, J. Nocedal, and R. A. Waltz, "KNITRO: An integrated package for nonlinear optimization," *Large-Scale Nonlin. Optimiz.*, pp. 35–59, 2005.
[43] A. Wachter and L. T. Biegler, "On the implementation of a primal-dual interior point filter line search algorithm for large-scale nonlinear programming," *Math. Program.*, vol. 106, no. 1, pp. 25–57, 2006.
[44] W. E. Hart, C. Laird, J.-P. Watson, and D. L. Woodruff, *Pyomo – Optimization Modeling in Python*. New York, NY, USA: Springer, 2012.
[45] Gurobi Documentation: Release 5.6, Gurobi Optimization, Inc., 2014.
[46] CPLEX Documentation: Release 12.4, IBM Corp., 2014.
[47] R. D. Zimmerman, C. E. Murillo-Sánchez, and R. J. Thomas, "MATPOWER: Steady-state operations, planning and analysis tools for power systems research and education," *IEEE Trans. Power Syst.*, vol. 26, no. 1, pp. 12–19, Feb. 2011.
[48] P. Lipka, R. O'Neill, and S. Oren, "Developing Line Current Magnitude Constraints for IEEE Test Problems," Tech. Rep., FERC, 2013.
[49] F. Palacios-Gomez, L. Lasdon, and M. Engquist, "Nonlinear optimization by successive linear programming," *Manage. Sci.*, vol. 28, no. 10, pp. 1106–1120, 1982.
[50] MATLAB, Version 8.3.0.532 (R2014a), The MathWorks Inc., 2014.
[51] R. Fletcher, S. Leyffer, and P. Toint, On the Global Convergence of an SLP-Filter Algorithm, Univ. Dundee, Dept. Math., U.K., 1998, Numerical Analysis Rep. NA/183.

Anya Castillo (S'12) holds a B.S. in Electrical and Computer Engineering and a Minor in Computer Science from Carnegie Mellon University and a M.S. from the Technology and Policy Program at Massachusetts Institute of Technology. She is currently pursuing a Ph.D. in Energy Economics and Operations Research from the Department of Geography and Environmental Engineering at the Johns Hopkins University, Baltimore, MD.

Her research interests are in power systems modeling, engineering economics, and regulatory affairs.

Paula Lipka (M'15) received a B.S. in Engineering from Harvey Mudd College, California, in 2008 and a M.S. in Industrial and Operations Engineering in 2009 from University of Michigan-Ann Arbor. She is currently pursuing a Ph.D. in the Industrial Engineering and Operations Research Department at University of California-Berkeley.

Her research interests are in transmission modeling, transmission switching, renewable energy, and energy markets.

Jean-Paul Watson (M'10) holds B.S., M.S., and Ph.D. degrees in Computer Science.

He is a Distinguished Member of Technical Staff in the Discrete Math and Optimization Department at Sandia National Laboratories in Albuquerque, New Mexico. He leads a number of research efforts related to stochastic optimization, ranging from fundamental algorithm research and development, to applications including power grid operations and planning.

Shmuel S. Oren (F'02) received the B.Sc. and M.Sc. degrees in Mechanical Engineering from the Technion Haifa, Israel, and the M.S. and Ph.D. degrees in Engineering Economic Systems from Stanford University.

He is Professor of IEOR at the University of California at Berkeley and holds the Earl J. Isaac Chair. He is also the Berkeley site director of the Power Systems Engineering Research Center (PSERC) and is a former member of the California ISO Market Surveillance Committee.

Dr. Oren is a Fellow of INFORMS.

Richard P. O'Neill (M'14) received the B.S. degree in Chemical Engineering and the Ph.D. degree in Operations Research from the University of Maryland at College Park.

He is the Chief Economic Advisor in the Federal Energy Regulatory Commission (FERC), Washington, DC.

Dr. O'Neill is a Fellow of INFORMS.